

with only thioether sulfur and imidazole nitrogen coordination. Although both pentacoordinate geometries have been found before for copper(II) complexes, this is the first reported example of the isolation and structural characterization of both square-pyramidal and trigonal-bipyramidal coordination geometries for the same complex.

Acknowledgment. We gratefully acknowledge support for this work by the U.S. Public Health Service, National Institutes of Health (Grant No. HL15104). The crystal structures were done at the Molecular Structure Laboratory of the University of Arizona.

Supplementary Material Available: Tables of final atom positional and thermal parameters, bond distances, and bond angles for both the green and blue forms of $[\text{CuL}_3](\text{BF}_4)_2$ (8 pages). Ordering information is given on any current masthead page.

Department of Chemistry
The University of Arizona
Tucson, Arizona 85721

Richard S. Glass*
Mahmood Sabahi
Massoud Hojjatie
George S. Wilson

Received November 17, 1986

Electrocatalytic Reduction of HSO_3^- to H_2S Based on a Water-Soluble Iron Porphyrin

Sir:

The reduction of HSO_3^- to H_2S occurs in nature via a stepwise, catalytic process that is carried out by the sulfite reductase enzymes.¹ They contain an iron isobacteriochlorin prosthetic group, which is known to bind sulfite. We have recently shown that the water-soluble iron porphyrin $[\text{Fe}^{\text{III}}(\text{TPPS})(\text{H}_2\text{O})_n]^{3+}$ ($n = 1$ or 2 ; TPPS = *meso*-tetrakis(*p*-sulfonatophenyl)porphine)² mimics the action of the enzyme nitrite reductase in its ability to reduce NO_2^- to NH_3 catalytically.^{3,4} We report here that the same iron porphyrin complex is also an effective electrocatalyst for the reduction of HSO_3^- to H_2S and that possible mechanistic insight into the reduction can be gained from the results of electrochemical studies on the reduction of $[\text{Ru}^{\text{II}}(\text{NH}_3)_5(\text{SO}_2)]^{2+5}$ to $[\text{Ru}^{\text{II}}(\text{NH}_3)_5(\text{H}_2\text{S})]^{2+6}$ where the sulfur ligand remains bound through the net six-electron change. The iron porphyrin appears to be the first example of a well-defined chemical system for the catalytic reduction of HSO_3^- to H_2S .

In Figure 1 is shown a cyclic voltammogram⁷ of $[\text{Ru}^{\text{II}}(\text{NH}_3)_5(\text{SO}_2)]^{2+}$ at pH 2.00. The wave at $E_{1/2} = +0.26$ V (vs. SCE) arises from the pH-dependent $[\text{Ru}^{\text{III}}(\text{NH}_3)_5(\text{HSO}_3)]^{2+}/[\text{Ru}^{\text{II}}(\text{NH}_3)_5(\text{SO}_2)]^{2+}$ couple.⁸ The process occurring at $E_{p,a} = +1.15$ V is an irreversible oxidation to give $[\text{Ru}^{\text{III}}(\text{NH}_3)_5(\text{SO}_4)]^{2+}$, as shown chemically by Isied and Taube.⁹ However, of more interest is the appearance of the multielectron, irreversible reduction at $E_{p,c} = -0.74$ V. Electrolysis^{10a} at $E_{\text{appl}} = -0.75$ V (appl

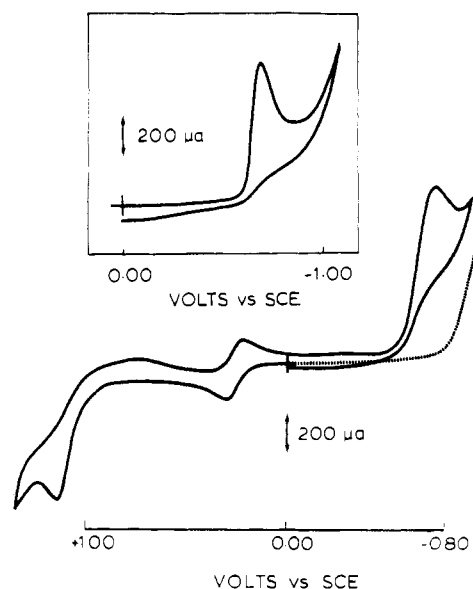


Figure 1. Cyclic voltammogram of a solution containing 1.3×10^{-3} M $[\text{Ru}^{\text{II}}(\text{NH}_3)_5(\text{SO}_2)]^{2+}$ at pH 2.0 in a 0.1 M sulfate buffer at a scan rate of 100 mV/s. The wave at $E_p = -0.74$ V is also observed if the scan is begun in the negative direction; the dashed curve shows the reductive background. The surface area of the glassy carbon electrode was 7.1 mm^2 . Inset: Cyclic voltammogram of 9.9×10^{-4} M $[(\text{NH}_3)_5\text{Ru}^{\text{II}}\text{SSRu}^{\text{III}}(\text{NH}_3)_5]^{4+}$, which is the initial reduction product, at pH 2.0 in a 0.1 M sulfate buffer at a scan rate of 100 mV/s.

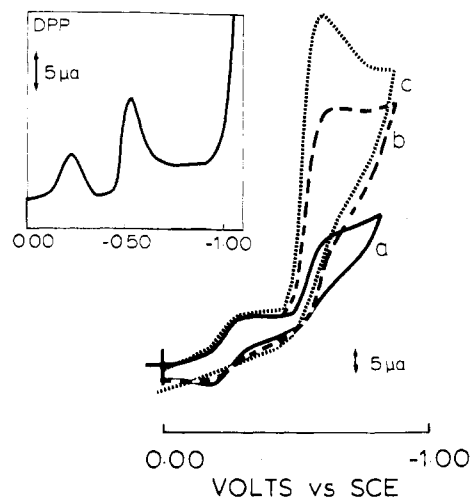


Figure 2. (a) Cyclic voltammogram of a solution containing 1.6×10^{-3} M $[\text{Fe}^{\text{III}}(\text{TPPS})(\text{H}_2\text{O})_n]^{3-}$ and a less than stoichiometric amount of HSO_3^- (1×10^{-3} M) in a phosphate buffer (0.1 M KH_2PO_4 with 0.6 M Na_2SO_4 added) at pH 3.48 at a scan rate of 50 mV/s. (b, c) Cyclic voltammograms of solutions 1.6×10^{-3} M in $[\text{Fe}^{\text{III}}(\text{TPPS})(\text{H}_2\text{O})_n]^{3-}$ containing 3.0×10^{-3} and 6.0×10^{-3} M HSO_3^- , respectively, at pH 3.48 in a phosphate buffer (0.1 M KH_2PO_4 with 0.6 M Na_2SO_4 added) at a scan rate of 50 mV/s. The surface area of the glassy carbon electrode was 7.1 mm^2 . Inset: Differential-pulse polarogram of a solution containing 2.0×10^{-3} M $\text{Na}_2\text{S}_2\text{O}_3$ and 7.6×10^{-4} M $[\text{Fe}^{\text{III}}(\text{TPPS})(\text{H}_2\text{O})_n]^{3-}$ at pH 2.74 (0.1 M phosphate buffer with 0.6 M Na_2SO_4 added); the scan rate is 10 mV/s.

= applied) until the initial current falls to $\sim 15\%$ of its initial value occurs with $n = 3.60 (\pm 0.06)$ per monomer to give $[(\text{NH}_3)_5\text{Ru}^{\text{III}}\text{SSRu}^{\text{III}}(\text{NH}_3)_5]^{4+}$ nearly quantitatively, as shown by spectral and electrochemical comparisons with a known sample prepared by the reaction between $[\text{Ru}^{\text{II}}(\text{NH}_3)_5(\text{SO}_2)]^{2+}$ and $\text{H}_2\text{S}(\text{g})$.¹¹ The cyclic voltammogram of the dimer at pH 2 is shown as an inset in Figure 1. The dimer itself undergoes an additional, kinetically slower reduction at the electrode at E_{appl}

- (1) Postgate, J. R. In *Inorganic Sulfur Chemistry*; Nickless, G., Ed.; Elsevier: New York, 1968; Chapter 8, pp 259-279.
- (2) Taniguchi, V. T. Ph.D. Dissertation, University of California, Irvine, CA, 1978.
- (3) Barley, M. H.; Takeuchi, K. J.; Murphy, W. R., Jr.; Meyer, T. J. *J. Chem. Soc., Chem. Commun.* **1985**, 507-508.
- (4) Barley, M. H.; Takeuchi, K. J.; Meyer, T. J. *J. Am. Chem. Soc.* **1986**, *108*, 5876-5885.
- (5) Gleu, K.; Rehm, K. Z. *Anorg. Allg. Chem.* **1938**, *235*, 211-219.
- (6) Kuehn, C. G.; Taube, H. *J. Am. Chem. Soc.* **1976**, *98*, 689-702.
- (7) All cyclic voltammetry experiments were performed with a glassy-carbon working electrode, a platinum-wire auxiliary electrode, and a saturated calomel (SCE) reference electrode.
- (8) Gleu, K.; Rehm, K. Z. *Anorg. Allg. Chem.* **1938**, *235*, 211-219.
- (9) Isied, S. S.; Taube, H. *J. Am. Chem. Soc.* **1973**, *95*, 8198-8200.
- (10) (a) All coulometric reductions were performed with a reticulated-carbon working electrode, a platinum-gauze auxiliary electrode, and a saturated calomel reference electrode. (b) The electrolyses were carried out to $n > 5$ with the initial current having fallen to 15-20% of its initial value. The value of n greater than the expected value of $n = 4$ for the $[(\text{NH}_3)_5\text{Ru}^{\text{III}}\text{SSRu}^{\text{III}}(\text{NH}_3)_5]^{2+} \rightarrow 2[\text{Ru}(\text{NH}_3)_5(\text{SH}_2)]^{2+}$ reduction and the continuing background current are probably the result of the catalytic production of H_2 by the complex.^{6,12}

- (11) Brulet, C. R.; Isied, S. S.; Taube, H. *J. Am. Chem. Soc.* **1973**, *95*, 4758-4759.

= -0.75 V. Reduction past $n > 5^{10b}$ per dimer occurs to give $[\text{Ru}^{\text{II}}(\text{NH}_3)_5(\text{H}_2\text{S})]^{2+}$ in high yield, as shown by the peak current of the wave for the $[\text{Ru}^{\text{III}}(\text{NH}_3)_5(\text{SH})]^{2+}/[\text{Ru}^{\text{II}}(\text{NH}_3)_5(\text{SH}_2)]^{2+}$ couple at $E_{1/2} = -0.42$ V ($E_{p,c} = -0.48$ V; $E_{p,a} = -0.36$ V vs. SCE)¹² in the cyclic voltammogram after the electrolysis. From cyclic voltammetric measurements under a variety of conditions, it is clear that the reduction of $[\text{Ru}^{\text{II}}(\text{NH}_3)_5(\text{SO}_2)]^{2+}$ occurs via at least one observable intermediate and that kinetic effects at the electrode are important.

The electrochemical results based on $[\text{Ru}^{\text{II}}(\text{NH}_3)_5(\text{SO}_2)]^{2+}$ are striking in showing the existence of a stepwise, net six-electron reduction of $[\text{Ru}^{\text{II}}(\text{NH}_3)_5(\text{SO}_2)]^{2+}$ to $[\text{Ru}^{\text{II}}(\text{NH}_3)_5(\text{H}_2\text{S})]^{2+}$ with retention of the initially bound sulfur, at least in the net sense, and in showing the importance mechanistically of intermediate S-S coupling. The ruthenium complex is not an effective catalyst under these conditions, because of the relatively high affinity of ruthenium for sulfur in both oxidation states +IV and -II.

In Figure 2 are shown cyclic voltammograms and a differential-pulse polarogram¹³ of solutions containing both $[\text{Fe}^{\text{III}}(\text{TPPS})(\text{H}_2\text{O})_n]^{3+}$ and less than stoichiometric HSO_3^- (curve a) at pH 3.48 and 2.74, respectively. As shown in Figure 2, a new, irreversible wave appears at $E_{p,c} = -0.64$ V with added HSO_3^- , which increases in peak current and becomes catalytic as the concentration of HSO_3^- is increased. As shown in Figure 2, the peak current for the wave at -0.64 V increases linearly with $[\text{HSO}_3^-]$ in the concentration range shown (curves b and c). A series of electrolysis experiments were carried out just past the wave at $E_{p,c} = -0.64$ V at $E_{\text{appl}} = -0.65$ V (pH 3.00). In a typical experiment a solution containing 4.6×10^{-3} M HSO_3^- and 1.2×10^{-4} M $[\text{Fe}^{\text{III}}(\text{TPPS})(\text{H}_2\text{O})_n]^{3+}$ at pH 3.5 was electrolyzed to $n = 3.9$ per added HSO_3^- to give H_2S in yields up to 52% of the initial HSO_3^- based on GC and gravimetric analysis.¹⁴ The background current in the absence of catalyst was negligible. Yields of less than 100% H_2S are expected under our conditions since an unavoidable complication in solutions containing high initial concentrations of HSO_3^- is the competitive formation of elemental sulfur formed by reaction between H_2S and HSO_3^- , which limits the yield of H_2S . Nonetheless, under the conditions of the experiment, H_2S was formed with a faradaic efficiency of 80%. The turnover number based on the total reductive equivalents passed was 170 or based on the moles of H_2S produced per mole of catalyst was 19.

Differential-pulse polarography and cyclic voltammetry experiments on the iron porphyrin in the presence of HSO_3^- (Figure 2) show that the new wave at $E_p = -0.64$ V appears following the reduction of Fe(III) to Fe(II) at $E_p = -0.23$ V. Presumably, reduction of Fe(III) to Fe(II) is followed by formation of an $\text{Fe}^{\text{II}}-\text{SO}_2$ or $\text{Fe}^{\text{II}}-\text{SO}_3\text{H}$ complex and the reduction at -0.64 V corresponds to the first stage of the net electrocatalytic reduction of bound HSO_3^- to H_2S . SO_2 complexes of Fe(II) porphyrins have been reported.¹⁵

In earlier work on the reduction of nitrile/nitrosyl to ammonia, coordinatively stable polypyridyl complexes of Ru provided useful insight into the probable mechanistic details by which the catalytically active iron porphyrins accomplish the net redox change.¹⁶ The pentaammineruthenium(II) system may serve that role here as well. pH-dependent electrochemical studies show that the SO_2 complex, $[(\text{NH}_3)_5\text{Ru}(\text{SO}_2)]^{2+}$, is the reactive form toward re-

duction, and the key to its reactivity may be the availability of low-lying levels, largely $\pi^*(\text{SO}_2)$ in character, which provide a basis for the initial reduction.¹⁷ In the electrochemistry of $[\text{Fe}^{\text{III}}(\text{TPPS})(\text{H}_2\text{O})_n]^{3+}$ in the presence of $\text{SO}_2/\text{HSO}_3^-$, the irreversible reduction at -0.64 V is analogous to the initial reduction of $[\text{Ru}^{\text{II}}(\text{NH}_3)_5(\text{SO}_2)]^{2+}$ at -0.74 V. The wave at -0.64 V for the porphyrin complex only appears in acidic solutions where at least small amounts of SO_2 are present and the active form of the porphyrin in the catalytic system appears to be an SO_2 complex as well. As shown by the cyclic voltammetric scans in Figure 2, the net turnover of SO_2 to H_2S is rapid. With less than excess added HSO_3^- (curve a), scan reversal past the $\text{HSO}_3^-/\text{SO}_2 \rightarrow \text{H}_2\text{S}$ electrocatalyzed reduction gives back the aqua couple, suggesting that $\text{HSO}_3^-/\text{SO}_2 \rightarrow \text{H}_2\text{S}$ reduction and subsequent axial displacement of bound H_2S by water are both rapid. As shown by the dashed curves in the figure (curves b and c), in the presence of excess HSO_3^- , scan reversal shows a greatly diminished Fe(III/II) aqua wave, suggesting that reduction, loss of H_2S , and re-formation of the active $\text{HSO}_3^-/\text{SO}_2$ complex are all rapid on the cyclic voltammetric time scale of 50 mV/s.

Acknowledgment is made for support of this research by the National Institutes of Health under Grant 5-RO1-GM32296-04.

(17) Ryan, R. R.; et al. *Struct. Bonding (Berlin)* 1981, 46, 46-97.

Department of Chemistry
The University of North Carolina
Chapel Hill, North Carolina 27514

Martha A. Kline
Mark H. Barley
Thomas J. Meyer*

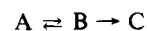
Received December 9, 1986

Uncomplexed Rather Than the Metal Ion Complexed α, α' -Carbanion as an Intermediate in Transamination between Pyridoxal and Pyridoxamine Schiff Bases

Sir:

A recent communication to the editor of this journal stated that an Al(III) α, α' -deprotonated complex is "a mandatory intermediate for the transamination process leading from ketimine to aldimine".¹ With a starting solution containing pyridoxamine, pyruvate, and Al(III) in a 1:1:1 ratio, Figure 2 in ref 1 shows the ¹H NMR evidence for buildup of an intermediate with a maximum concentration at about 2 h and, separately, continuous production of aldimine as the main product of the reaction. However, the continuous increase does not conform to the requirements for a consecutive reaction sequence in which the intermediate lies on the reaction pathway from reactants to aldimine. Instead the results fit a competitive reaction scheme in which the presumed intermediate appears as a metastable byproduct produced in a reversible side reaction that does not lie on the reaction pathway from reactants to aldimine.

The proposed sequence of reactions in the consecutive reaction scheme may be represented as



where A represents the reactants, B, the intermediate whose concentration builds and then declines, and C, aldimine as the main product of the reaction. Figure 2 of ref 1, however, does not display the required characteristics for consecutive reactions. Though there is a buildup and decline of an intermediate, the maximum alone is insufficient to establish an intermediate in a consecutive reaction sequence. The intensity vs. time curve for the aldimine product must display an induction period with an inflection point occurring at the same time as the maximum in the curve for the intermediate.² The aldimine curve in ref 1 shows no clear induction period, and the required inflection point is

(12) Kuehn, C. G. Ph.D. Dissertation, Stanford University, Stanford, CA, 1975; p 63.

(13) Single-sweep voltammetry and differential-pulse polarography experiments were performed with a glassy-carbon working electrode, a platinum-wire auxiliary electrode, and a saturated calomel reference electrode.

(14) GC analysis was performed by using an HP-5890 gas chromatograph and a Chromosorb 107, 80/100 Teflon column. Gravimetric analysis was performed by precipitation and weighing of $\text{ZnS} \cdot \text{H}_2\text{O}$ formed in a trap past the electrolysis cell. The H_2S formed during electrolysis was transferred to the trap by a continuous Ar purge. The trap contained 0.1 M zinc acetate dihydrate.

(15) Kuroi, T.; Nakamoto, K. *J. Mol. Struct.* 1986, 146, 111-121.

(16) Murphy, W. R., Jr.; Takeuchi, K. J.; Barley, M. H.; Meyer, T. J. *Inorg. Chem.* 1986, 25, 1041-1053.

(1) Martell, A. E.; Taylor, P. *Inorg. Chem.* 1984, 23, 2734.

(2) Martin, R. B. *J. Chem. Educ.* 1985, 62, 789.